Explanation of the mechanism of destruction of the cylindrical sample in the Brazilian test *

Conference Paper · September 2015

DOI: 10.1201/b20057-102

2 authors:


Podgórski Jerzy
Lublin University of Technology


Gontarz Jakub
Lublin University of Technology

Explanation of the mechanism of destruction of the cylindrical sample in the Brazilian test*

Jakub Gontarz[1] and Jerzy Podgórski[2]

[1] *Faculty of Civil Engineering and Architecture, Lublin University of Technology*
Nadbystrzycka 40, 20-618 Lublin, Poland
e-mail: j.podgorski@pollub.pl

[2] *Faculty of Civil Engineering and Architecture, Lublin University of Technology*
Nadbystrzycka 40, 20-618 Lublin, Poland
e-mail: j.gontarz@pollub.pl

Abstract

The paper presents the analysis of the so-called Brazilian compression tests of the cylinder loaded by the two linearly distributed balanced forces, in terms of possibility of determining the proper tensile strength of the material. These analyses contain the precisely determined stress field, without the singularity at the point of force application, the determination of the critical stress from the point of view of the classical and contemporary failure criteria for the brittle materials, and the position of the point at which the destructive crack may start to destroy the sample. The classical mechanism of the destruction relies on the analysis of the plane stress state which requires revision and its replacement with a 3D model. These analyses are supported by experimental data from own laboratory tests.

Keywords: Brazilian test, concrete mechanics, rock mechanics, failure criteria, material effort ratio

The paper presents a study of the indirect method of determining the tensile strength of brittle materials such as concrete and rocks. This type of test is mostly performed using the “Brazilian” method, by compressing the cylinder on the lateral surface with two linear balancing loads. The simplicity of this test and the convenience of using the core drilling as laboratory samples, made the “Brazilian” method a dominant attempt to determining the tensile strength of natural rocks and concrete. The strength of the material in the sample is usually determined by taking the maximum tensile stress, attained at the time of failure, as a measure of this characteristic of the material. This stress is mostly determined by considering the two dimensional task of theory of elasticity for circular disc which is in a flat state of stress, compressed by the two balancing forces applied along the diameter, which gives:

$$f_t = \frac{2P_{\max}}{\pi\, d\, h}\,, \tag{1}$$

where P_{max} is a destructive force of sample, d - diameter and h - height of the tested cylinder.

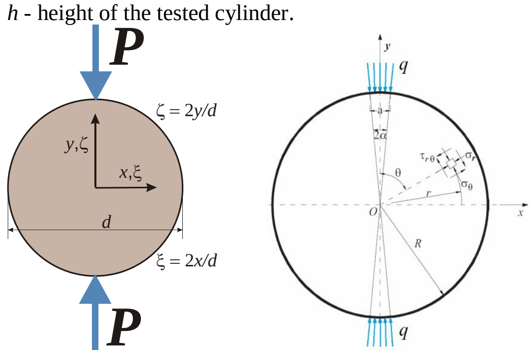

a) b)

Figure 1: The issue of circular disc compression – Brazilian test, a) concentrated force, b) distributed load by. Hondros

Tensile strength, determined in this way, has values lower than that determined on a direct tensile test. The reason for this are excessive simplifications of determining the stress field and neglecting the impact of compressive stress, which have a significant impact on the effort of material.

The problem of determining the material strength and modulus of elasticity basing on the results of the measurements made during the Brazilian test is still an interesting topic of research, which can be observed in many studies appearing in scientific journals dedicated to the problems of rock mechanics and concrete [1,2,3].

The authors of this study have attempted to accurately determine the tensile strength obtained in Brazilian test by analyzing the material effort basing on modern and conventional failure conditions applicable for concrete and natural rocks. The conditions Lame-Rankine, Mohr-Coulomb, Drucker-Prager, Ottosen-Podgorski were analyzed.

1. Stress field

Determination of stress values in compression along the circular disc diameter (Fig. 1) is a classic issue, solved at the end of XIX century by Flamand and Hertz [4].

The equations of the stress tensor components in the Cartesian coordinate system can be expressed as follows [4,5]:

$$
\begin{aligned}
\sigma_x &= \frac{-2P}{\pi\, d\, h}\left[\frac{(1-\zeta)\xi^2}{\left((1-\zeta)^2+\xi^2\right)^2}+\frac{(1+\zeta)\xi^2}{\left((1+\zeta)^2+\xi^2\right)^2}-\frac{1}{2}\right]\\
\sigma_y &= \frac{-2P}{\pi\, d\, h}\left[\frac{(1-\zeta)^3}{\left((1-\zeta)^2+\xi^2\right)^2}+\frac{(1+\zeta)^3}{\left((1+\zeta)^2+\xi^2\right)^2}-\frac{1}{2}\right]\\
\tau_{xy} &= \frac{-2P}{\pi\, d\, h}\left[\frac{(1-\zeta)^2\xi}{\left((1-\zeta)^2+\xi^2\right)^2}+\frac{(1+\zeta)^2\xi}{\left((1+\zeta)^2+\xi^2\right)^2}\right]
\end{aligned} \tag{2}
$$

Figure 2 shows a map of stress fields in areas corresponding to quarter of the compressed cylinder in the case of the graph σ_x,

*This research was sponsored by the statutory fund of the Faculty of Civil Engineering and Architecture, Lublin University of Technology.

and half of the cylinder in the case of compressive stress σ_y and tangential τ_{xy}.

As it can be seen, in the middle section ($\xi = 0$, $\zeta = 0$) compressive stresses σ_y are in absolute value three times greater than the tensile stresses σ_x ($\sigma_y/\sigma_x = -3$). In applying point of concentrated force, there are singularities of both the stress fields because $\sigma_y \to -\infty$, $\sigma_x \to \infty$. Graphs of the stresses in section where $x = 0$ are shown in Fig. 3a.

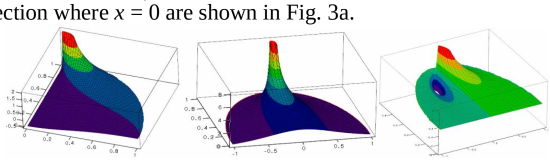

σ_x σ_y τ_{xy}

Figure 2. Stress distribution in the circular disc compressed with concentrated forces

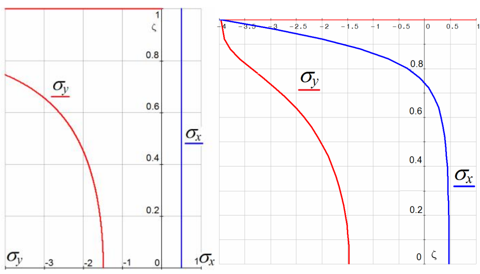

a) b)

Figure 3. Charts of stresses σ_x and σ_y in section $x = 0$, a) for the concentrated load, b) distributed load

In the real task for a cylinder, the stress field singularities do not exist, because the force always have to be applied as a pressure on a small area of the lateral surface (Fig. 3b). Field of the stresses in this case has been designated by Hondros [1, 6] as the series:

$$\sigma_r = -\frac{2q}{\pi}\left\{\alpha + \sum_{n=1}^{\infty}\left[1-\left(1-\frac{1}{n}\right)\left(\frac{r}{R}\right)^2\right]\left(\frac{r}{R}\right)^{2n-2}\sin 2n\alpha\ \cos 2n\theta\right\}$$
$$\sigma_\theta = -\frac{2q}{\pi}\left\{\alpha - \sum_{n=1}^{\infty}\left[1-\left(1+\frac{1}{n}\right)\left(\frac{r}{R}\right)^2\right]\left(\frac{r}{R}\right)^{2n-2}\sin 2n\alpha\ \cos 2n\theta\right\} \quad (3)$$
$$\tau_{r\theta} = -\frac{2q}{\pi}\left\{\sum_{n=1}^{\infty}\left[1-\left(\frac{r}{R}\right)^2\right]\left(\frac{r}{R}\right)^{2n-2}\sin 2n\alpha\ \sin 2n\theta\right\}$$

Figure 4**Błąd! Nie można odnaleźć źródła odwołania.** shows the isolines of stress field and Fig. 3b is a graph of stresses σ_x and σ_y in section x = 0 of circular disc loaded by pressure *p*, similar to the diagram of stresses induced by the concentrated force shown in Fig. 3a. A lack of singularity at the point of load application is visible here. In the case of a small width "*a*" of load pressure strip, the stress distribution in the center region of the disc is not significantly different from distribution σ_x and σ_y shown in Fig. 3a.

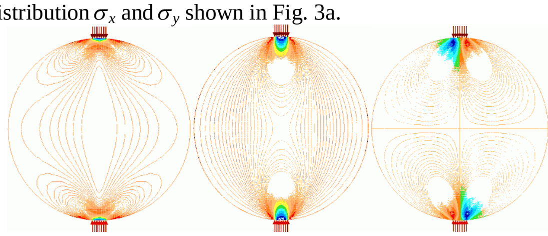

σ_x σ_y τ_{xy}

Figure 4. Isolines of stress tensor components for distributed load

2. Criteria for material damage

2.1. Lame-Rankine criterion

Lame and Rankine assumed that the excision of the biggest strength of the main stress determines the failure of the material:

$$f_c \le \sigma_1 \le f_t\,,\ \ f_c \le \sigma_2 \le f_t \quad (4)$$

The border envelope of this condition in the area of "compression-stretching" is shown in Fig. 5.

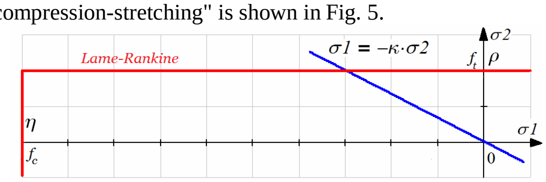

Figure 5. The envelope of Lame-Rankin condition

2.2. Coulomb-Mohr criterion

According to this hypothesis the maximum shear stress that exceeds the cohesive value enlarged by the friction force determines the failure of the material:

$$\tau_{\max} \le c - \sigma_n tg\phi\,, \quad (5)$$

In this equation σ_n is the stress normal to the plane τ_{max}, c is cohesive and ϕ is the angle of internal friction. The values of parameters c and tanϕ can be determined from known values of compressive strength - f_c and tensile strength - f_t.

$$c = \frac{f_c}{2(\eta+1)}\,,\quad tg\phi = \frac{\eta-1}{2(\eta+1)}\,,\quad \eta = f_c / f_t\,.$$

The boundary envelope of Coulomb-Mohr condition in the area $\sigma_1 \le 0$, $\sigma_2 \ge 0$ is shown in **Błąd! Nie można odnaleźć źródła odwołania.**.

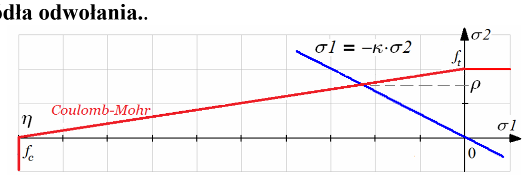

Figure 6. The envelope of Coulomb-Mohr condition

2.3. Drucker-Prager criterion

Drucker-Prager condition [7] is based on similar to Coulomb-Mohr dependence expressed in the form of invariants in an octahedral plane:

$$\tau_O \le c - b\,\sigma_O\,, \quad (6)$$

in this equation $\sigma_O = (\sigma_1+\sigma_2+\sigma_3)/3$ is the average normal stress, $\tau_O = \sqrt{\frac{2J_2}{3}}$ is the tangential octahedral stress, J_2 is the second invariant of stress deviator, c and b are constants that can be determined from known values of compressive strength - f_c and tensile strength - f_t.

$$c = f_c \frac{2\sqrt{2}}{3(\eta+1)}\,,$$

The envelope boundary of Drucker-Prager condition in the area $\sigma_1 \le 0$, $\sigma_2 \ge 0$ is shown in Fig.7.

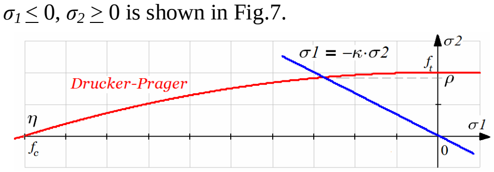

Figure 7. The envelope of Drucker-Prager condition

2.4. Ottosen-Podgórski (JP) criterion

Ottosen-Podgórski condition [7,8] has been proposed in the form which expresses the relationship of three alternative stress tensor invariants:

$$\sigma_0 - C_0 + C_1 P(J)\tau_0 + C_2\tau_0^2 = 0\,, \tag{7}$$

where $P(J)$ is a function describing the cross-section of limit state surface σ_O = const. Ottosen [9,10] proposed to adopt this function in the form: $P(J) = \cos\left(\frac{1}{3}\arccos\alpha\, J\right)$, analogous to the function generated by Lade and Matsuoka conditions [7]. Modification of this function by J. Podgórski [7,8] helped to better match the envelope of boundary surface with experimental data for concrete and also generalized the condition to include the classic Tresca and Coulomb-Mohr conditions: $P(J) = \cos\left(\frac{1}{3}\arccos(\alpha\, J) - \beta\right)$. In equation (7): $\sigma_0 = \frac{1}{3}I_1$, $\tau_0 = \sqrt{\frac{2}{3}J_2}$ were determined. I_1 - represents the first invariant of the stress tensor, J_2, J_3 - invariants of the stress deviator, α, β, C_0, C_1, C_2 - are constants dependent on the material. The proposed method of determining that constants is described in the author's earlier works [9,11]. The boundary surface of J. Podgórski condition and the envelope in 2D stress state are shown in Fig. 8.

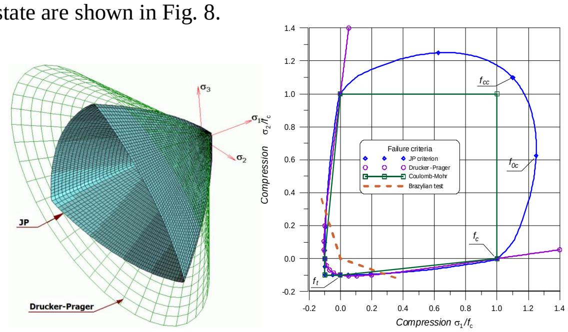

Figure 8. Boundary surface for J. Podgórski criterion and its envelope for 2D stress state σ_3=0.

2.5. Determination of tensile strength

Comparing the ordinate of the point of the load path intersection in the Brazilian test ($\sigma_1 = \kappa\cdot\sigma_2$) with the envelope of the material failure condition (Figures 5,6,7,8), it can be seen that only in the case of the simplest Lame-Rankine criterion the maximum tensile stress obtained with Brazilian test $\sigma_{\max} = \dfrac{2P_{\max}}{\pi\, d\, h}$ can be regarded as tensile strength, $f_t = \sigma_{max}$, in other cases there is always $f_t > \sigma_{max}$, which means $\rho = \dfrac{\sigma_{\max}}{f_t} < 1$.

For the circular disc loaded in the middle with a concentrated force the stress distribution can be obtained, which gives $\sigma_1 = \sigma_y$, $\sigma_2 = \sigma_x$, $\kappa = \dfrac{\sigma_1}{\sigma_2} = -3$. In the case of distributed load the value of coefficient κ is little different from 3,0. Seeking the point of intersection of lines $\sigma_2 = \dfrac{-\sigma_1}{\kappa}$ and $\sigma_2 = 1 + \dfrac{\sigma_1}{\eta}$ for the Coulomb-Mohr criterion we get:

$$\rho = \frac{\sigma_{\max}}{f_t} = \frac{1}{1+\gamma}\,,\ \text{where}\ \gamma = \frac{\kappa}{\eta}\,. \tag{8}$$

Taking $\kappa = 3{,}0$ and $\eta = 10$ we obtain: $f_t = (1+\gamma)\sigma_{\max} = 1{,}3\sigma_{\max}$, so the tensile strength for the material subjected to Coulomb-Mohr failure criterion should be 30% higher than the maximum tensile stress occurring in the Brazilian test.

In case of other criteria, to obtain such a simple relationship between σ_{max} and f_t as in equation (8) is not possible, but observing a small difference (Fig. 9) between the position of the envelope described by Drucker-Prager and *JP* conditions and the parabola of the equation $\dfrac{\sigma_2}{f_t} = 1 - \left(\dfrac{\sigma_1}{f_c}\right)^2$ it can be assume with sufficient accuracy that the intersection of the parabola with the load path in Brazilian test gives the wanted value for σ_{max}.

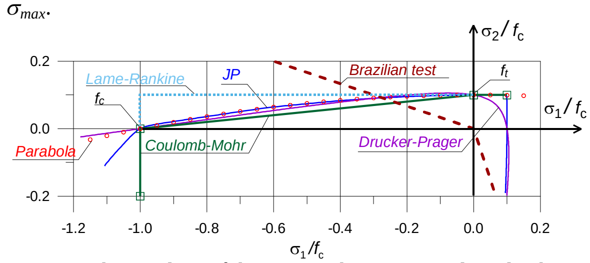

Figure 9. The envelope of the *JP*, Drucker-Prager and Coulomb-Mohr conditions on the plane σ_1 - σ_2

The breaking stress now can be received by using a simple relationship: $\sigma_{\max} = \rho \cdot f$, where:

$$\rho = \frac{\sqrt{1+4\gamma^2} - 1}{2\gamma^2}\,,\ \gamma = \frac{\kappa}{\eta}\,. \tag{9}$$

Taking again κ = 3,0 and η = 10 we get ρ = 0,92328, and the exact calculations for the Drucker-Prager condition give value ρ = 0,92332, which deviates less than $4\cdot 10^{-5}$ between that received from equation (9). The tensile strength calculated using the *JP* and Drucker-Prager conditions is therefore approx. 8% higher than the σ_{max}, which means that $f_t = \dfrac{\sigma_{\max}}{\rho} \approx 1{,}083\sigma_{\max}$.

3. The formation of a destructive crack

3.1. The criterion for crack initiation

As a criterion for crack initiation which starts the damaging process of the material we adopted the achievement of effort, which corresponds to the point in the stress space situated at the border surface defined by the equation (5), (6) or (7) depending on the taken condition of the failure. It was assumed that the loading of the sample increases monotonically and the failure process starts at a point where the effort reaches the maximum value. Effort (μ) of the material is defined as the ratio of modules of vectors r_σ and r_f:

$$\mu = \frac{|\mathbf{r}_\sigma|}{|\mathbf{r}_f|} = \frac{r_\sigma}{r_f}\,, \tag{10}$$

where r_σ is a vector indicating the point (in the stress space) according to the stress state in the analyzed place of the sample, and r_f is a vector indicating a point on the boundary surface, which also belongs to the path of monotonic load (Fig. 10).

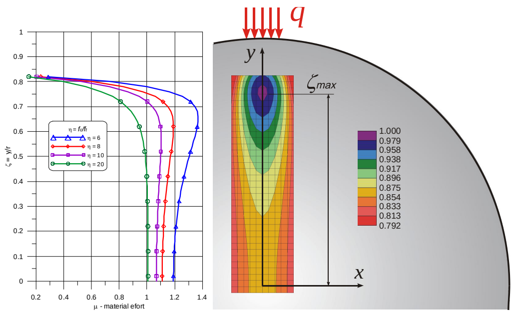

a) b)

Figure 10. Definition of the material effort coefficient μ, a) values of this coefficient on the axis of the sample compressed with a distributed load depending on the ratio of strength η, b) map of the effort coefficient μ according to *PJ* criterion, determined on the FEA numerical analysis.

3.2. Location of crack initiation

Effort of the sample material determined in accordance with equation (10), after adopting the stress field described by Hondros equations (2), in points lying on the axis $x = 0$ is shown in **Błąd! Nie można odnaleźć źródła odwołania.**a. Here is used a parabolic approximation of Drucker-Prager and Ottosen-Podgórski conditions, setting effort curves for different ratios $\eta = f_c/f_t$. It is visible that the displacement of the point of maximal effort from the center of the sample, which can be seen for large η values, to the loaded edge of the sample with η values lower than 15. The location of this point is defined with a dimensionless coordinate ζ_{max} for different effort hypotheses for a fixed $\eta = 10$, and is shown in Table 1. In addition, there is also given the coefficients $\kappa = \sigma_1/\sigma_2$ and ρ determined in accordance with equation (9).

Table 1. Comparison of efforts depending on the criterion of failure, the $\eta = 10$

Failure criterion	Concentrated force			Distributed load		
	$\zeta_{\max}$	$\kappa = \sigma_1/\sigma_2$	ρ	$\zeta_{\max}$	$\kappa = \sigma_1/\sigma_2$	ρ
Coulomb-Mohr	0	3	0,769	0,593	5,167	0,659
Drucker-Prager	0	3	0,923	0,566	4,885	0,834
Ottosen-Podgórski	0	3	0,923	0,566	4,885	0,834
Parabolic envelope	0	3	0,923	0,566	4,885	0,834
Lame-Rankine	0	3	1,0	0	3,112	1,0

4. Summary and conclusions

The paper presents a study of the indirect method of determining the tensile strength of brittle materials known as the "Brazilian" method, by compressing the cylinder on the lateral surface with two linear balancing loads. The strength of the material in the sample is usually determined by taking the maximum tensile stress, attained at the time of failure, as the value of this characteristic. Such estimates are usually adopted in standard for building industry and for laboratory testing [12,13,14]. As it was shown, this stress is significantly lower than the breaking stress of the sample in a state of pure unidirectional stretching. These differences can be estimated on the assumed condition of failure in a 3D state of stress. Basing on the results of analyzes of material effort, we can assume that this difference is approx. 8%, while taking the Drucker-Prager and Ottosen-Podgórski conditions, and can reach up to 30%, while taking the Coulomb-Mohr condition.

An interesting issue is also the location of the place of initiation of a destructive crack. As shown in the graphs of material effort, the place of maximal effort depends on the ratio $\eta = f_c/f_t$. When $\eta < 17$, a point of crack initiation moves toward the loaded edge of the sample and when $\eta \geq 17$ the maximal effort point is located in the center of the sample.

The real mechanism of destruction of the sample is different and its explanation requires taking take into account the spatial work of the sample material. The corresponding analysis performed by finite element method taking into account the JP fracture criterion and triaxial stress state, explains the mechanism of destruction and indicates the origin of the destructive crack (Fig. 11).

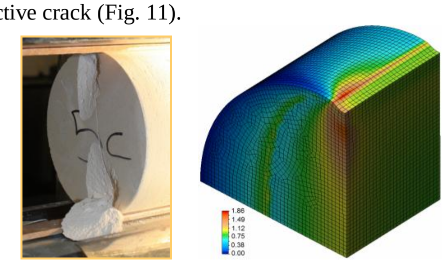

a) b)

Figure 11. View of destroyed sample after the Brazilian test (a) and map of effort coefficient calculated for 3D FEM model (b).

Table 2. Position of the point of maximal effort, depending on the relative of strength $\eta = f_c/f_t$

η	5	7	10	13	15	16	17	20
$\zeta_{\max}$	0,668	0,638	0,566	0,439	0,293	0,170	0,0	0,0

5. References:

1 Ye Jianhong, F. Q. Wu, J. Z. Sun, *Estimation of the tensile elastic modulus using Brazilian disc..*, Int. Journ. Rock Mechanics & Mining. Sciences 46 (2009) 568–576.

2 Nihal Aréoglu, Z. Canan Girgin, and Ergin Aréoglu, *Evaluation of Ratio between Splitting Tensile Strength..*, ACI Materials Journal, V. 103, No. 1, Jan. 2006, 18-24.

3 C. S. Chen and S. C. Hsu, *Measurement of Indirect Tensile Strength of Anisotropic Rocks by the Ring Test*, Rock Mech. Rock Engng. (2001) 34 (4), 293-321.

4 S. Timoshenko, J. N. Goodier, *Theory of elasticityi*, Arkady, Warszawa 1962.

5 N. I. Mushelishvili, *Nekotorye Osnovnye Zadachi Matematicheskoj Teorii Uprugosti*., Nauka, Moskwa 1949

6 G. Hondros, *The evaluation of Poisson's ratio and the modulus of mat...*, Aust. J. Appl. Sci. 1959, 10, 243-268.

7 J. Podgórski, *Limit state condition and the dissipation function for isotropic materials*, Archives of Mechanics, 36(1984)3, 323-342.

8 J. Podgórski, *General Failure Criterion for Isotropic Media*. Journ. Eng. Mech. ASCE, 111(1985)2, 188-201.

9 J. Podgórski, *Limit state condition and the dissipation function..*, Archives of Mechanics, 36(1984)3, 323-342.

10 N. S. Ottosen, *A Failure Criterion for Concrete*, Journ. Eng. Mech., ASCE, Vol. 103, No. EM4, Aug., 1977, pp. 527-535.

11 J. Podgórski, *Criterion for angle prediction for the crack..*, Mechanics and Control vol 30, No 4 (2011), 229-233.

12 Norma PN-EN 12390-6:2011, *Wytrzymałość na rozciąganie przy rozłupywaniu próbek do badań*,Polish Standard

13 *Test method T222. Indirect tensile strength of rock drill core..*, NSW Roads and Maritime Services, Australia

14 *Standard Test Method for splitting Tensile Strength of Intact Rock Core Specimens*, ASTM Standards, USA